Available online at www.sciencedirect.com
SCIENCE DIRECT®
Deep-Sea Research I 51 (2004) 999–1015
DEEP-SEA RESEARCH PART I
www.elsevier.com/locate/dsr

Simple models of steady deep maxima in chlorophyll and biomass

Benjamin A. Hodges*, Daniel L. Rudnick

Scripps Institution of Oceanography, University of California, San Diego, Mail Code 0213, La Jolla, CA 92093-0213, USA

Received 18 March 2003; received in revised form 1 October 2003; accepted 17 February 2004

Abstract

Possible mechanisms behind the observed deep maxima in chlorophyll and phytoplankton biomass in the open ocean are investigated with simple, one-dimensional ecosystem models. Sinking of organic matter is shown to be critical to the formation of a deep maximum in biomass in these models. However, the form of the sinking material is not of primary importance to the system: in models with sinking of detritus, sinking of one phytoplankton species, and sinking of all phytoplankton, the effect is qualitatively the same. In the two-compartment nutrient-phytoplankton model, the magnitude of the deep biomass maximum depends more strongly on sinking rate and diffusivity than on growth and death rates, while the depth of the maximum is influenced by all four parameters. A model with two phytoplankton groups which exhibit distinct growth rate characteristics and chlorophyll contents shows how a deep chlorophyll maximum could form in the absence of sinking. In this model, when separate compartments are included for nitrate and ammonia, it is possible to distinguish between new and regenerated production, and the phytoplankton group which makes up the deep chlorophyll maximum is found to carry out almost all of the new production. Variation of eddy diffusivity with depth is also investigated, and is found not to fundamentally alter results from models with constant diffusivity.

Keywords: Deep chlorophyll maximum; Phytoplankton; Nutrients; Models

1. Introduction

The deep chlorophyll maximum (DCM) is a ubiquitous feature of many regions of the world's oceans (Venrick et al., 1973; Cullen, 1982). As fluorescence is perhaps the most easily measured biological oceanic variable, the DCM is the most widely known feature of the ocean ecosystem. A permanent characteristic throughout much of the tropics, deep chlorophyll maxima are also familiar features in temperate regions, although usually subject there to strong seasonal variability (Venrick, 1993; Winn et al., 1995).

Deep maxima in phytoplankton biomass are also common. Such a deep biomass maximum (DBM) is evident in the tropical eastern Pacific

*Corresponding author. Tel.: +1-858-822-1278; fax: +1-858-534-8045.
E-mail address: bhodges@ucsd.edu (B.A. Hodges).

0967-0637/$ - see front matter © 2004 Elsevier Ltd. All rights reserved.
doi:10.1016/j.dsr.2004.02.009

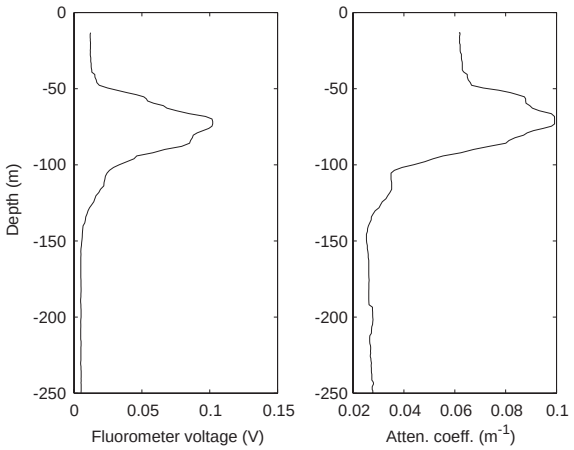

Fig. 1. Vertical profiles of chlorophyll *a* fluorescence and beam attenuation coefficient of 660 nm light, a rough measure of POC. The component of attenuation due to absorption by water has been removed. The measurements were made on October 4, 2001, at 5.5°N, 95.4°W, as part of EPIC-2001.

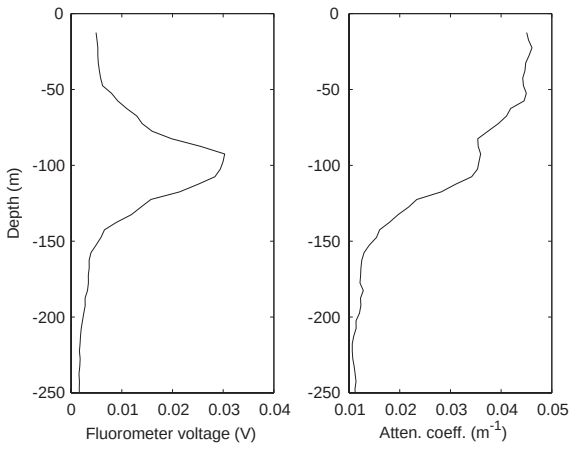

Fig. 2. Vertical profiles of chlorophyll *a* fluorescence and beam attenuation coefficient. The data were obtained during the HOME 2002 experiment on October 15, 2002, at latitude 21°N, longitude 159°W.

at 5.5°N (Fig. 1). Shown here are typical profiles of in vivo fluorescence of chlorophyll *a*, an approximate measure of chlorophyll concentration (Lorenzen, 1966), and beam attenuation coefficient, an approximate measure of particulate organic carbon (POC) (Bishop, 1999). Prominent deep maxima are evident in both. A DCM often occurs without an accompanying DBM, however (Winn et al., 1995). This is due to variation in the chlorophyll-to-biomass ratio, which may vary by as much as a factor of 10 (Cullen and Lewis, 1988). The effect is exemplified in typical profiles of fluorescence and beam attenuation coefficient from the tropical Pacific near Hawaii (Fig. 2). While a strong DCM is present, there is no significant deep maximum apparent in POC. A DBM is not implied by the existence of a DCM, and when both are present they often differ in vertical structure (Kitchen and Zaneveld, 1990; Fennel and Boss, 2003), so it is important to distinguish between the two signatures. On the other hand, since the chlorophyll-to-biomass ratio generally increases with depth in the euphotic zone, the presence of a DBM does typically imply a DCM, and any mechanism which causes the former also causes the latter.

A number of mechanisms have been proposed for the formation of deep maxima, and indeed it seems likely that a variety of effects are involved. In a recent paper, Fennel and Boss (2003) investigate the separation of the DCM and DBM, and possible causes of each. Efforts to model the DCM date back to 1949, when Riley, Stommel, and Bumpus tackled the problem in their seminal paper. Several fairly complex models of the planktonic ecosystem exist (e.g. Jamart et al., 1977; Varela et al., 1992), which are able to accurately match observations. Rather than striving to reproduce precisely the features of a specific set of observations, the aim of this paper is to use simple, one-dimensional ecosystem models to examine the feasibility of a few basic mechanisms which might give rise to deep maxima in chlorophyll and biomass.

The models presented here are closed, in the sense that there is no exchange of material across the model domain boundaries. Since there are essentially no live phytoplankton deeper than a few hundred meters, most models have been limited to this region. However, nutrient profiles have typically not reached their asymptotic, deep-ocean values at the bottom of this layer, so these models include an upward diffusive flux of

nutrients through the bottom boundary of their domain. The magnitude of this flux depends on the position of the bottom boundary, and on the boundary conditions. As our goal is to understand how vertical distributions of phytoplankton and variables relevant to their ecosystem arise, we extend our models to a depth great enough to ensure that all model variables attain their asymptotic values.

The models are kept as simple as possible, allowing isolation of the most fundamental processes underlying the complex ecological system. We subscribe to Occam's razor, which suggests that the simplest explanation of a phenomenon is intrinsically best. In addition, a sufficiently simple model allows a full search of parameter space, permitting a more complete understanding of the mathematical system than would be possible in models of higher complexity.

2. Basic assumptions

It is convenient and sensible to deal in some currency when modeling the plankton ecosystem. The most common choice, and the one we make here, is nitrogen (e.g. Steele, 1974) because it is assumed to be the limiting nutrient of photosynthetic growth. Thus, $P(z)$ represents the concentration of phytoplankton as a function of depth in terms of the nitrogen it contains. Minimizing the number of other forms (compartments) in which the currency can exist is essential if one hopes to form a simple model. So we begin, in our simplest models, without a zooplankton compartment; rather than being modelled explicitly, the effects of grazing are included in the net phytoplankton growth rate. Similarly, we begin with the assumption that all phytoplankton exhibit the same environment-dependent rates of biological activity, and none of our models include more than two such phytoplankton groups.

There are several other significant simplifications in our models. Each variable is treated as a continuum, whereas, of course, real plankton are discrete (see, e.g. Young, 2001). Only one spatial dimension is modeled (the vertical). Thus, such phenomena as horizontal patchiness in the distribution of phytoplankton (see Denman et al., 1977 for a discussion) and the horizontal transport of plankton and nutrients are not considered. Though the ocean is a time-dependent environment, we consider only the steady-state solutions to the models. As the DCM is a permanent feature of large regions of the ocean, it seems reasonable to regard the changes it undergoes as fluctuations about a steady-state distribution. The models' intrinsic time scales, determined by the rates of biological activity and by diffusion and sinking, coupled with the attenuation length of light, are all of the order of tens of days for the parameter ranges considered. The steady solution applies if it has been at least this long since a major perturbation in the system. Modeled light intensity depends only on depth (i.e. there is no self-shading) and no other properties (except, sometimes, turbulent diffusivity) are explicit functions of depth. The only process which is directly affected by light is photosynthetic growth, so depth dependence of chlorophyll-to-nitrogen ratio, remineralization rate, zooplankton grazing rate, etc. is not included. The reasoning behind this choice is that allowing explicit vertical variation in more processes would introduce additional degrees of freedom to the modeling problem, clouding understanding of the mechanisms at work.

3. How simple is too simple?

One popular explanation of the deep maxima is outlined by Mann and Lazier (1996) in their recent textbook: "…a certain amount of nitrate is transported upward through the nutricline by turbulent diffusion. This process leads to more rapid growth of the phytoplankton population and the formation of a zone of maximum phytoplankton biomass, the 'chlorophyll maximum', just above the nutricline. The upper boundary of this zone is set by the supply of nutrients from below, and the lower boundary is set by the availability of light from above". A simple model simulating the process described in the above explanation would have two compartments: phytoplankton P and nutrients N. The net rate at which nitrogen flows from N to P may be represented by $\mu(N, P, z)$,

where z, the vertical coordinate, is zero at the surface and increases upward.[1] $\mu(N,P,z)$ is the rate of total phytoplankton growth minus all losses, including those due to death. If we denote the turbulent diffusivity by $\kappa(z)$, we obtain the model equations

$$\frac{\partial N}{\partial t} = -\mu(N,P,z) + \frac{\partial}{\partial z}\left(\kappa\frac{\partial N}{\partial z}\right), \tag{1}$$

$$\frac{\partial P}{\partial t} = \mu(N,P,z) + \frac{\partial}{\partial z}\left(\kappa\frac{\partial P}{\partial z}\right), \tag{2}$$

with the boundary conditions

$$\frac{\partial N}{\partial z} = \frac{\partial P}{\partial z} = 0 \text{ at } z = 0,$$
$$N = 1, \quad P = 0 \text{ at } z = -\infty.$$

The bottom boundary conditions reflect the normalization of N and P such that the deep nutrient concentration is 1. That is, the dimensional concentrations of nutrients and phytoplankton have been divided by the concentration of nitrogen at great depth, which we take to be 10 μmol l^{-1} (Edwards et al., 2000), so that N and P are unitless. The surface boundary conditions are chosen so as to make the diffusive flux of N and P through the surface zero.

In this model, growth of plankton uses up nutrients, and when plankton die they are immediately converted back into dissolved nutrients. As we are interested in the steady-state solution, we set the time derivatives of N and P equal to zero and solve the system numerically using Newton's method. In seeking the steady solution, we are assuming that such a solution exists and is stable. The assumption of existence is justified once a solution is found, and stability is proven in the Appendix. Although we do not prove explicitly that the models presented in later sections have stable solutions, stability is favored by the diffusive nature of the models. Stability of models of this type has been examined by a number of authors (Criminale and Winter, 1974; Lima et al., 2002; Edwards et al., 2000).

The system described above appears reasonable, and certainly it is simple, but it can be shown that this system cannot yield a realistic deep maximum in P. In order to show this, we first define $S = N + P$ to be the total concentration of nitrogen in any form. It is easy to solve for S: by adding Eqs. (1) and (2), we obtain

$$\frac{\partial}{\partial z}\left(\kappa\frac{\partial S}{\partial z}\right) = 0. \tag{3}$$

Transforming the boundary conditions gives $\partial S/\partial z = 0$ at $z = 0$ and $S = 1$ at $z = -\infty$; the solution is $S(z) = 1$. Thus $N + P = 1$ and any deep maximum in P must accompany a deep *minimum* in N; that is, a deep phytoplankton maximum and a nutricline cannot coexist. This result is neither dependent on the form of the growth rate term nor on the behavior of diffusivity with depth. In order to understand the mechanisms behind a steady DBM, it is necessary to look beyond this simple model and the explanation it represents.

However, solutions to this over-simplified model provide a useful reference against which to compare results from more realistic models. To obtain these solutions we must choose functional forms for the growth and diffusivity terms. Since nutrients and light are both necessary for photosynthetic growth, the rate at which P grows should be an increasing function of N, and an increasing function of light intensity, PAR(z) (photosynthetically active radiation). If we take these functions to be as simple as possible, i.e. assume linear proportionality, we arrive at $\widetilde{\mathrm{G}}N[\mathrm{PAR}(z)]$ as the growth rate, where $\widetilde{\mathrm{G}}$ is a constant. Assuming K, the attenuation coefficient of PAR(z), is constant with depth, $\mathrm{PAR}(z) = \mathrm{e}^{\mathrm{K}z}\mathrm{PAR}(0)$. Defining $\mathrm{G} \equiv \widetilde{\mathrm{G}}/\mathrm{PAR}(0)$, our growth rate is $\mathrm{G}N\mathrm{e}^{\mathrm{K}z}$.

Note that the values assigned to G, sometimes as large as 100 day^{-1}, may appear at first to be unrealistically high, but that to get a growth rate of G, nutrient concentration and light level would both have to reach their maximum values (1 in both the cases) at the same location. As light level is maximum at the surface and nutrient concentration is maximum at great depth, this never

[1] Our convention, throughout this work, will be to use italic capital Roman letters for nitrogen compartments, italic lowercase Roman letters for independent variables, Greek letters for parameters which may be functions of independent variables or compartments, and normal-text capital Roman letters for other (constant) parameters.

happens, and the actual phytoplankton growth rate is always much less than G.

Following the Michaelis–Menten equation, a growth rate with a half-saturation dependence on nutrient or light levels is perhaps more traditional in this kind of model (Jamart et al., 1977; Franks et al., 1986; Fasham et al., 1990). However, the euphotic ocean operates mostly at low N, where saturation is irrelevant, and we have found that such elaborations change the solutions only slightly. We have therefore opted for simplicity. Adding a constant specific death rate, D (which includes respiration as well as grazing and other modes of physiological death), and taking diffusivity to be constant with depth, we obtain the system

$$\frac{\partial N}{\partial t} = -\mathrm{G}NP\mathrm{e}^{\mathrm{K}z} + \mathrm{D}P + \kappa\frac{\partial^2 N}{\partial z^2}, \tag{4}$$

$$\frac{\partial P}{\partial t} = \mathrm{G}NP\mathrm{e}^{\mathrm{K}z} - \mathrm{D}P + \kappa\frac{\partial^2 P}{\partial z^2}, \tag{5}$$

with the same boundary conditions as before.

A steady deep phytoplankton maximum is not consistent with this system, because any such maximum would have to occur in a location darker and poorer in nutrients, and therefore with a slower growth rate, than the surface. A typical solution is shown in Fig. 3. The parameter values are $\mathrm{G} = 20\ \mathrm{day}^{-1}$, $\mathrm{D} = 0.1\ \mathrm{day}^{-1}$, and $\kappa = 10^{-4}\ \mathrm{m}^2\ \mathrm{s}^{-1}$. The phytoplankton maximum is, as it must be, at the surface. In the model equations above, the bottom boundary condition is applied at $z = -\infty$, but for computational purposes, we apply this condition at a finite depth deep enough that change with depth has ceased; in this case the bottom boundary is at 800 m. Note that in Fig. 3 and subsequent figures, only the surface region of this model domain is depicted, so that near-surface behavior may be more clearly seen.

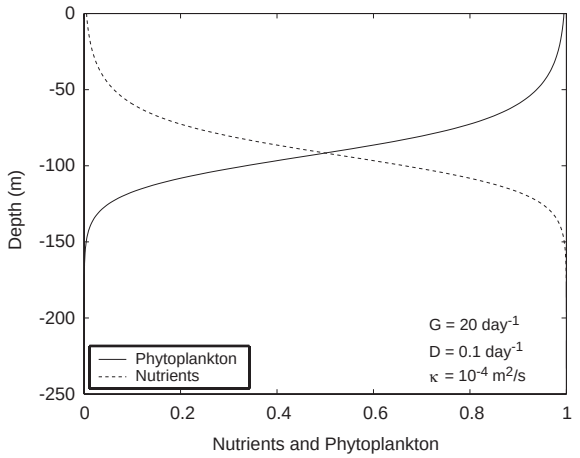

Fig. 3. Solution to the NP model without sinking, Eqs. (4) and (5), for the parameter values shown. The profiles of nutrients (dashed) and phytoplankton are mirror images of each other.

4. Sinking of phytoplankton

Deep biomass maxima do exist in many areas, particularly in the tropics. In order to simulate the DBM with our model, the total amount of nitrogen in the surface layer must be depleted. The simplest mechanism that can maintain a depletion against the homogenizing effect of diffusion is the sinking of nitrogen. Accordingly, we introduce a constant phytoplankton sinking rate. The modified system is

$$\frac{\partial N}{\partial t} = -\mathrm{G}NP\mathrm{e}^{\mathrm{K}z} + \mathrm{D}P + \kappa\frac{\partial^2 N}{\partial z^2}, \tag{6}$$

$$\frac{\partial P}{\partial t} = \mathrm{G}NP\mathrm{e}^{\mathrm{K}z} - \mathrm{D}P + \kappa\frac{\partial^2 P}{\partial z^2} - \mathrm{W}\frac{\partial P}{\partial z}, \tag{7}$$

with the boundary conditions

$$\kappa\frac{\partial N}{\partial z} = \mathrm{W}P - \kappa\frac{\partial P}{\partial z} = 0 \text{ at } z = 0,$$

$$N = 1, \quad P = 0 \text{ at } z = -\infty.$$

W is the sinking rate, and the surface boundary condition on P has been changed so that the total flux of phytoplankton (diffusive plus sinking) through the surface is zero. The solution has a marked increase in phytoplankton concentration from the surface to the deep maximum, due to the nitrogen depletion of the surface caused by sinking of phytoplankton (Fig. 4). As long as the chlorophyll-to-biomass ratio is constant or increasing with depth, this DBM is also a DCM. Of the four terms in the P equation above (Eq. (7)), the dominant balance throughout the euphotic zone is between growth and death (Fig. 5(a)). However, as growth and death only move nitrogen

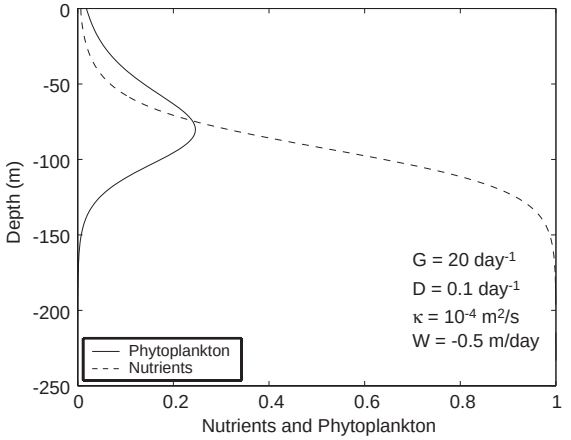

Fig. 4. Solution to the NP model with sinking, Eqs. (6) and (7). Note the pronounced deep maximum in phytoplankton.

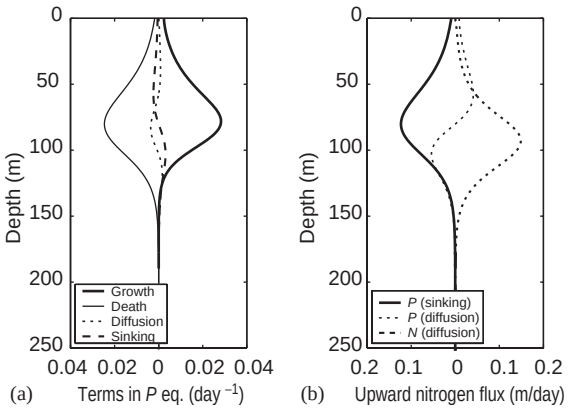

Fig. 5. (a) The terms in Eq. (7) plotted versus depth for the model solution in Fig. 4. The four terms sum to zero, and the dominant balance in the euphotic zone is between growth and death. (b) Vertical flux balance for the same solution. Units on the horizontal axes reflect the fact that nitrogen concentration has been nondimensionalized.

from one compartment to the other, they do not directly affect the profile of total nitrogen ($N + P$). It is a balance between sinking and diffusion that determines this profile. The flux of total nitrogen must be zero everywhere, so the downward flux of nitrogen due to the sinking of P is balanced by an upward diffusive flux of total nitrogen

$$-\kappa\frac{\partial N}{\partial z} - \kappa\frac{\partial P}{\partial z} + \mathrm{W}P = 0. \tag{8}$$

This flux balance is illustrated in Fig. 5(b), which shows as functions of depth the vertical diffusive flux of nutrients (the first term in (8)) and phytoplankton (the second term), and the vertical flux of phytoplankton due to sinking (the third term). Sinking of phytoplankton rains nitrogen out of the surface layer, and diffusion works to replenish it.

The model, in the form above, includes five variable parameters: $\mathrm{G}, \mathrm{D}, \kappa, \mathrm{K}$, and W. We now nondimensionalize the system by scaling the vertical coordinate, z, by the attenuation length, K^{-1}, and dividing Eqs. (6) and (7) by D, the death rate. (Note that the variables N and P are already nondimensional, having been scaled by the limiting nutrient value at depth.) After making the following substitutions:

$$z^* \leftarrow \mathrm{K}z,$$
$$t^* \leftarrow t\mathrm{D},$$
$$\mathrm{G}^* \leftarrow \mathrm{G}/\mathrm{D},$$
$$\mathrm{W}^* \leftarrow \mathrm{W}\mathrm{K}/\mathrm{D},$$
$$\kappa^* \leftarrow \kappa\mathrm{K}^2/\mathrm{D}$$

and dropping the asterisks, the nondimensional system obtained looks exactly like the dimensional system above, except that K and D are equal to unity. The full parameter space of this model therefore has only three dimensions, and is investigated rather easily.

Numerical solutions were obtained for the region of parameter space defined by the (dimensional) values in Table 1. A DBM is a feature in solutions to the system throughout this entire region. For particularly small sinking velocity and large diffusivity, the surface concentration of phytoplankton approaches that at the deep

Table 1
The region of parameter space for which numerical solutions to the NP model with sinking (Eqs. (6) and (7)) were obtained

Parameter	Symbol	Value range	Unit
Attenuation coefficient	K	0.05	m
Death rate	D	0.1	day^{-1}
Growth rate	G	2.5–62.5	day^{-1}
Diffusivity	κ	$(5\text{–}125)\times10^{-5}$	$\mathrm{m}^2\ \mathrm{s}^{-1}$
Sinking velocity	W	2.5–0.1	$\mathrm{m\ day}^{-1}$

maximum. In these cases, diffusion dominates, and the sinking is not able to deplete the total nitrogen in the surface layer. In the limit as the ratio $W/K\kappa$ approaches zero, the model reduces to the trial system of Section 3, and the plankton maximum is at the surface.

Phytoplankton concentration and the depth of the deep maximum vary considerably across the explored block of G–κ–W parameter space. Each contour plot in Fig. 6 represents a two-dimensional slice through the three-dimensional parameter space. Because small diffusivities and fast sinking rates deplete the surface layer of nitrogen, they lead to small phytoplankton concentrations which peak well below the surface; larger diffusivities and slower sinking rates yield larger

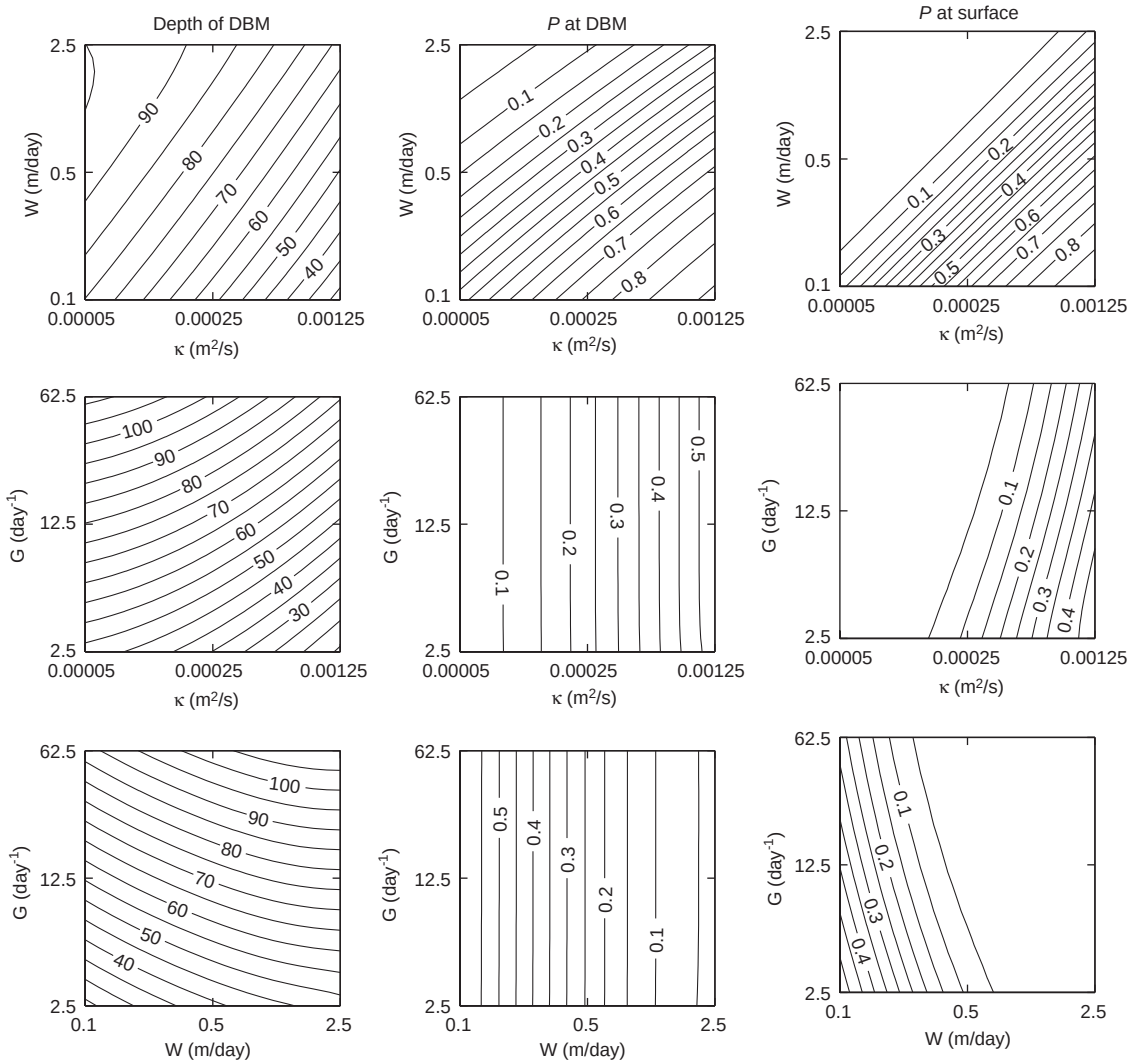

Fig. 6. Behavior of the phytoplankton profile produced by the NP model with sinking (Eqs. (6) and (7)) as a function of position in G–κ–W parameter space. Depth of the DBM in meters is plotted in the left-hand column, phytoplankton concentration P at the maximum in the middle column, and phytoplankton concentration at the surface in the right-hand column. The dimensional parameter values corresponding to these figures are $D = 0.1\ day^{-1}$, and $K = 0.05\ m^{-1}$. In the upper panels G is constant at $27\ day^{-1}$; in the middle panels W is constant at $-1\ m\ day^{-1}$; and in the bottom panels, κ is constant at $10^{-4}\ m^2\ s^{-1}$. Note the logarithmic scaling of the axes.

phytoplankton concentrations with shallower maxima (Fig. 6, top row).

At the surface, phytoplankton concentration is determined by the extent of the surface nitrogen depletion. The depletion is most complete, and hence the surface value of P is smallest, when W is large and κ is small (Fig. 6, right-hand column). Though the dependence is weak, P at the surface decreases with increasing growth rate (G), because faster-growing phytoplankton are more efficient at depleting surface nitrogen.

The phytoplankton concentration at the deep maximum is not a function of G (note the vertical contour lines in the lower two panels of the middle row in Fig. 6). The axes in Fig. 6 are scaled logarithmically. As indicated by the even spacing in the G direction of the contours in the lower two panels of the left-hand column in Fig. 6, the depth of the deep maximum is proportional to the logarithm of G. Any vertical line drawn from top to bottom across either of these panels represents a range of G from 2.5 to 62.5 day^{-1}, and spans about 64 m (3.2/K) of depth contours.

If the sinking flux of phytoplankton is sufficient to deplete the surface layer of nitrogen, as it is throughout most of our parameter space, $P(z=0)$ will be small. Using this fact, we can infer the effect of varying the value of G, and understand the behavior observed in Fig. 6. Consider the NP system with sinking (Eqs. (6) and (7)) after nondimensionalizing and making the substitutions $z \to z' + \mathrm{H}$ and $\mathrm{G} \to \mathrm{G}'\mathrm{e}^{-\mathrm{H}}$:

$$\frac{\partial N}{\partial t} = -\mathrm{G}' N P \mathrm{e}^{z'} + P + \kappa \frac{\partial^2 N}{\partial z'^2}, \tag{9}$$

$$\frac{\partial P}{\partial t} = \mathrm{G}' N P \mathrm{e}^{z'} - P + \kappa \frac{\partial^2 P}{\partial z'^2} - \mathrm{W} \frac{\partial P}{\partial z'}, \tag{10}$$

with the boundary conditions

$$\kappa \frac{\partial N}{\partial z'} = \mathrm{W}P - \kappa \frac{\partial P}{\partial z'} = 0 \text{ at } z' = -\mathrm{H},$$

$$N = 1, \quad P = 0 \text{ at } z' = -\infty.$$

This system looks very similar to the original one. The only thing stopping us from concluding that changing G just amounts to shifting the vertical coordinate is that the surface boundary condition is applied at $z' = -\mathrm{H}$, rather than $z' = 0$. Now, under the assumption that P is small near the surface, (9) and (10) may be approximated in the surface region by

$$\kappa \frac{\partial^2 N}{\partial z'^2} \approx 0,$$

$$\kappa \frac{\partial^2 P}{\partial z'^2} \approx \mathrm{W} \frac{\partial P}{\partial z'}.$$

Integrating these from $z' = -\mathrm{H}$ to 0, and applying the BC's for $z' = -\mathrm{H}$, we find

$$\kappa \frac{\partial N}{\partial z'} \approx \mathrm{W}P - \kappa \frac{\partial P}{\partial z'} \approx 0 \text{ at } z' = 0,$$

which suggests that applying the boundary conditions at $z' = 0$ provides a reasonable approximation. Thus if $P(z=0)$ is small, the approximate solution for $\mathrm{G} = \mathrm{X}\mathrm{G}_0$, where X is an arbitrary constant, may be obtained from the solution for $\mathrm{G} = \mathrm{G}_0$ by shifting it upward by the amount $\Delta z = -\ln(\mathrm{X})$. This explains why the magnitude of the maximum is not a function of G, and why the depth of the maximum changes by about 3.2 attenuation lengths when the value of G changes by a factor of 25: $\ln(25) \approx 3.2$.

Though we have scaled the parameter D out of our model equations by nondimensionalization, and hence it is not varied in our study of parameter space, we can still consider the effect of varying the death rate in the original, dimensional NP model with sinking. Referring back to that system, Eqs. (6) and (7), we can see that the solution for the parameter set $\{\mathrm{G}, \mathrm{W}, \kappa, \mathrm{D}\}$, where $\mathrm{D} = \mathrm{X}\mathrm{D}_0$, is the same as the solution for the parameter set $\{\mathrm{G}/\mathrm{X}, \mathrm{W}/\mathrm{X}, \kappa/\mathrm{X}, \mathrm{D}_0\}$. Since we have a solution set for a single death rate, D_0, we can see the result of increasing (decreasing) the death rate by a given factor by decreasing (increasing) the other parameters by that same factor. So, for example, since we know that the phytoplankton concentration at the DBM does not depend on G, we can infer the dependence of this magnitude on death rate from Fig. 6, middle panel, top row. Changing D corresponds to moving along lines which run across this figure from lower left to upper right at an angle of 45°. As the contours themselves are nearly parallel to these lines, the phytoplankton concentration at the

maximum is only weakly affected by the value of the death rate.

In the NP model with sinking, the magnitude of the phytoplankton concentration is largely a function of the physical variables κ and W and not of the biological variables G and D (although the sinking rate, W, is certainly influenced by biology, we classify it as a physical variable because it depends directly on particle size and density). The biological variables are important, however, in determining the depth of the DBM. As the contours in the lower two panels of the left-hand column of Fig. 6 are more nearly horizontal than vertical, the depth of the maximum depends more strongly on G than on either of the physical variables.

5. The effects of variable diffusivity

The eddy diffusivity, κ, is much larger within the mixed layer than beneath. It has occasionally been suggested that this transition could be important in the formation of a deep phytoplankton maximum. In this section, we explore the consequences of introducing a step-function diffusivity profile into the NP model with sinking from the previous section. The diffusive terms in the model equations are rewritten as $\partial/\partial z(\kappa\partial N/\partial z)$ and $\partial/\partial z(\kappa\partial P/\partial z)$, which are the valid forms when κ is a function of z.

The effect of introducing a 60-m-deep mixed layer to the model is shown in Fig. 7(a). The value of κ is increased by a factor of 10 in this mixed layer, but otherwise all parameter values are retained from Fig. 4. For comparison, the nutrient and plankton profiles for the constant-κ case are shown as dashed lines. The deep maximum is at a depth of approximately 85 m, and so is beneath the base of the mixed layer. While there are noticeable changes in the profile of phytoplankton within the mixed layer itself, in the deeper water the profile is essentially unaffected.

Next, consider the less typical case of a mixed layer whose base lies beneath the deep maximum. Fig. 7(b) shows the same 'reference' profiles as before together with the profiles obtained for the case of a 120-m mixed layer. Here, the diffusivity is

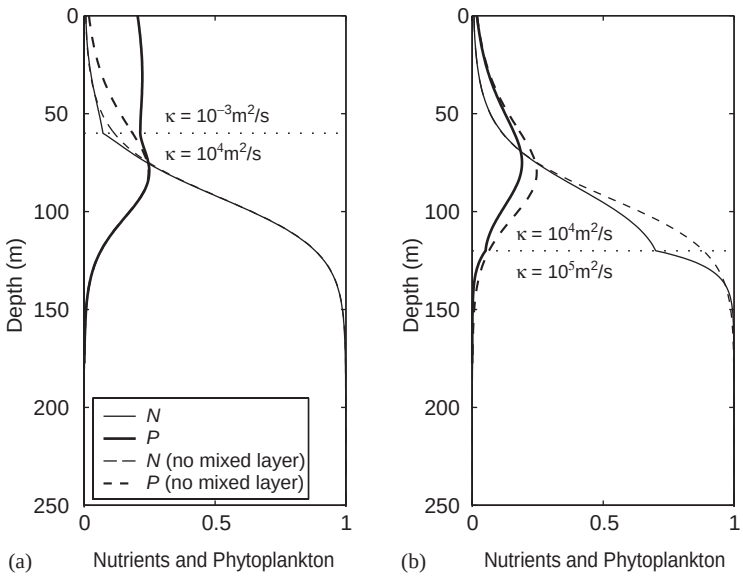

Fig. 7. Solutions to the NP model with sinking (Eqs. (6) and (7)) with mixed layers in the form of step-function diffusivity profiles. The thick lines are phytoplankton and the thin lines are nutrients. In (a), κ decreases from 10^{-3} to 10^{-4} m^2 s^{-1} at a depth of 60 m; in (b), κ decreases from 10^{-4} to 10^{-5} m^2 s^{-1} at a depth of 120 m. The other parameters retain their values from Fig. 4, from which the solutions are re-plotted (dashed lines) for comparison.

left unchanged within the mixed layer, but it is *decreased* by a factor of 10 below the mixed layer base. Maintaining the value of κ at the deep maximum at 10^{-4} m^2 s^{-1} in both cases allows the resulting profiles to be compared directly with the reference profile. Once again, the changes induced by the introduction of the mixed layer are relatively minor. Thus, in our simple models, the characteristics of the deep maximum depend in large part on the value of κ in the vicinity of the maximum, and only weakly on the behavior of the profile of κ at other depths.

6. A third compartment

We have emphasized that sinking is a crucial process in the formation of the DBM as represented in our simple model with only nutrient and phytoplankton compartments. The question remains, however, whether a deep phytoplankton maximum may result from a model without the surface-depleting effect of sinking, but with additional, nonphytoplankton nitrogen compartments. With this in mind, we introduce a third compartment, T, here a detrital pool. The new free parameter is a remineralization rate, R, which governs the transformation of detritus back into dissolved nutrients, parameterizing nutrient recycling via the microbial loop. The model equations are

$$\frac{\partial N}{\partial t} = -\mathrm{G}NP\mathrm{e}^{\mathrm{K}z} + \mathrm{R}T + \kappa\frac{\partial^2 N}{\partial z^2}, \tag{11}$$

$$\frac{\partial P}{\partial t} = \mathrm{G}NP\mathrm{e}^{\mathrm{K}z} - \mathrm{D}P + \kappa\frac{\partial^2 P}{\partial z^2}, \tag{12}$$

$$\frac{\partial T}{\partial t} = \mathrm{D}P - \mathrm{R}D + \kappa\frac{\partial^2 D}{\partial z^2}, \tag{13}$$

subject to the boundary conditions

$$\frac{\partial N}{\partial z} = \frac{\partial P}{\partial z} = \frac{\partial T}{\partial z} = 0 \text{ at } z = 0,$$

$$N = 1, \quad P = T = 0 \text{ at } z = -\infty.$$

Numerical simulations were carried out scanning a large physically and biologically reasonable region of parameter space similar to the one described for the two-compartment model in Section 4; κ varied from 10^{-5} to 10^{-2} m^2 s^{-1}, G varied from 1 to 100 day^{-1}, and the remineralization rate, R, took on values from 0.001 to 1.25 day^{-1}. While there is a region of this parameter space in which deep maxima do occur, the increase in phytoplankton concentration from the surface to the deep maximum is never as much as 3% of the deep nitrogen concentration. The strongest such maximum (i.e. the one with the greatest increase in phytoplankton concentration from the surface to the maximum) occurs when G = 100 day^{-1}, R = 0.0135 day^{-1}, and $\kappa = 0.00082$ m^2 s^{-1}, and is shown in Fig. 8.

The third compartment, T, could also be regarded as a zooplankton pool. In that case, D represents a constant (independent of T) grazing rate, and R a zooplankton loss rate, including death and excretion. Similar results are found when the grazing rate is linear in T (when the DP terms in the system above are replaced by DPT) unless the grazing rate is so large that no stable nontrivial solution exists. This suggests that, provided they have no explicit depth dependence, no number of additional compartments is likely to lead to the formation of a large and robust DBM in a simple one-dimensional ecosystem model without sinking.

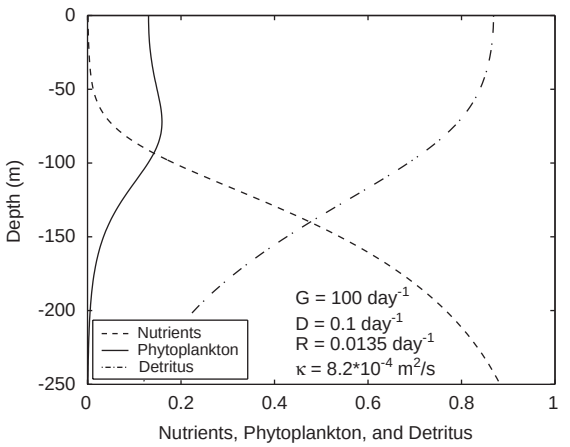

Fig. 8. Solution to the NPT model, which includes a detrital compartment but no sinking (Eqs. (11), (12), and (13)). In terms of increase in phytoplankton concentration relative to the surface, this deep maximum is the largest in the region of parameter space described in the text.

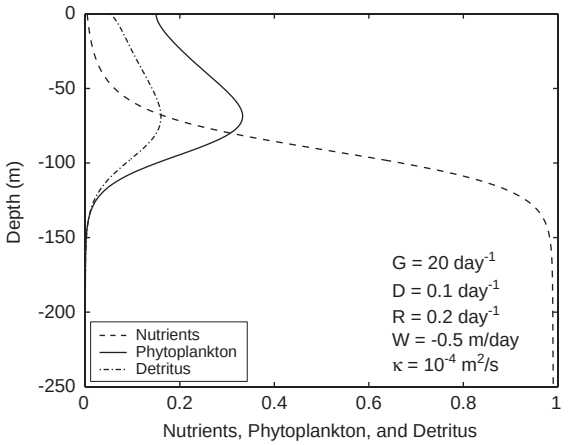

Fig. 9. Solution to the three-compartment NPT model with sinking of detritus. The remineralization rate, R, is 0.2 day^{-1}, and the other parameters are the same as in Fig. 4, to which this figure may be compared.

When sinking of detritus is included in the model above, its behavior is qualitatively very similar to that displayed by the two-compartment model with sinking from Section 4. Fig. 9 shows the solution for this case when the value of R is 0.2 day^{-1} and the rest of the parameter values are retained from Fig. 4. The phytoplankton and nutrient profiles are quite similar to those shown in Fig. 4; the biggest difference is that depletion of nitrogen in the surface layer is less effective in the three-compartment model. The sinking flux is smaller because only detritus sinks in this case and the concentration of detritus is smaller than is the concentration of phytoplankton in the NP model. The result is a higher concentration of phytoplankton at the surface. This slight difference is not due to any distinct effects of detrital sinking versus sinking of live phytoplankton. Of primary importance to the model ecosystem is only the magnitude of the sinking flux of organic matter, not the form that matter takes.

7. Multiple phytoplankton species

Though sinking is a prerequisite for the formation of a steady DBM in our NP model, variation with depth in the chlorophyll-to-biomass ratio can lead to a deep *chlorophyll* maximum. If photoadaptation is a dominant process in determining the distribution of chlorophyll—that is, if phytoplankton in deeper water develop significantly higher chlorophyll-to-biomass ratios in response to the low light intensity than do those near the surface—a strong DCM may form without a phytoplankton maximum. In fact, a DCM may form even in the absence of photoadaptation if multiple species of phytoplankton are considered, each with its own chlorophyll-to-biomass ratio and its own response to light level. Consider the simple NP system from Section 3 with constant κ and no sinking, but with phytoplankton split into two groups, P and Q. These groups will henceforth be referred to as 'species', with the understanding that each may actually represent an aggregate of many species with similar biological characteristics. The new system is

$$\frac{\partial N}{\partial t} = -\mathrm{G}_P N P \mathrm{e}^{\mathrm{K}z} + \mathrm{D}_P P - \mathrm{G}_Q N Q \mathrm{e}^{2\mathrm{K}z} + \mathrm{D}_Q Q + \kappa \frac{\partial^2 N}{\partial z^2}, \tag{14}$$

$$\frac{\partial P}{\partial t} = \mathrm{G}_P N P \mathrm{e}^{\mathrm{K}z} - \mathrm{D}_P P + \kappa \frac{\partial^2 P}{\partial z^2}, \tag{15}$$

$$\frac{\partial Q}{\partial t} = \mathrm{G}_Q N Q \mathrm{e}^{2\mathrm{K}z} - \mathrm{D}_Q Q + \kappa \frac{\partial^2 Q}{\partial z^2}, \tag{16}$$

with the boundary conditions

$$\frac{\partial N}{\partial z} = \frac{\partial P}{\partial z} = \frac{\partial Q}{\partial z} = 0 \text{ at } z = 0,$$

$$N = 1, \quad P = Q = 0 \text{ at } z = -\infty.$$

The specific growth rates of P and Q, $\mathrm{G}_P N \mathrm{e}^{\mathrm{K}z}$ and $\mathrm{G}_Q N \mathrm{e}^{2\mathrm{K}z}$, respectively, differ both in their surface values and in the way they decay with depth. The growth rate of P retains its linear dependence on light, and so has an e-folding length of K^{-1}. The growth rate of Q, on the other hand, is quadratic in light, and so has an e-folding length of $\frac{1}{2}\mathrm{K}^{-1}$; that is, Q's growth rate decays with depth twice as fast as that of P. The surface growth rate of Q, G_Q, is chosen to be larger than G_P. The result is that phytoplankton P is better adapted for high-nutrient, low-light environments, while Q is better adapted for low-nutrient, high-light ones. The

quadratic form of the growth rate of Q is chosen as a simple way to achieve this adaptive difference between P and Q. One factor which could contribute to differences in rates of decay of growth rates with depth is that the attenuation coefficient of light in sea water is frequency dependent, and the absorption spectrum of phytoplankton varies from species to species (Yentsch and Yentsch, 1979; Bricaud et al., 1983; Falkowski and Kiefer, 1985). This effect is relatively minor, however, and here, the dominant factor in the foreshortening of the growth rate profile is that phytoplankton Q functions less efficiently in lower-light conditions.

The system develops a pronounced deep maximum in P, the species that is better equipped to survive in dimmer light. The maximum concentration of Q occurs at the surface. Such vertical separations between different phytoplankton communities are consistent with observations (e.g. Venrick, 1993). Although the model still produces no DBM, a DCM may exist if the deeper species has a higher chlorophyll-to-biomass ratio, a reasonable assumption since a species which lives mainly in a low-light environment would need more chlorophyll. This effect is demonstrated in Fig. 10, in which plankton P has a chlorophyll-to-biomass ratio which is larger than that of plankton Q by a reasonable

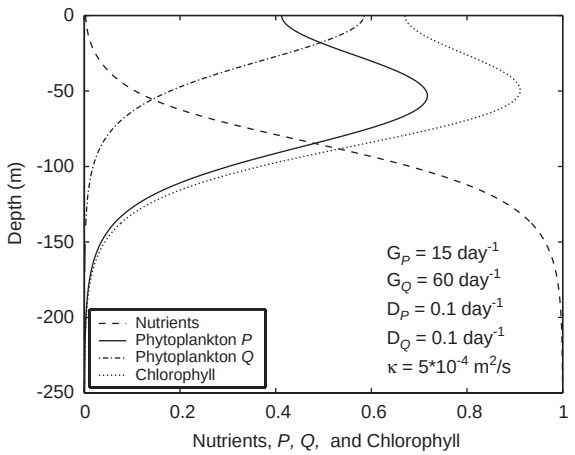

Fig. 10. Solution to the two-phytoplankton NPQ model, Eqs. (14), (15), and (16). The length scale of decay of the growth rate of plankton P is twice that of plankton Q, and P has a chlorophyll-to-biomass ratio four times as large as that of Q. Chlorophyll concentration is plotted with arbitrary units.

(Bricaud et al., 1983) factor of four. Biomass has been assumed, here, to be proportional to nitrogen content via its Redfield ratio to the other major elemental constituents of phytoplankton (Redfield et al., 1982). Photoadaptation within each species, if included in the model, would enhance this DCM. Thus the 'NPQ' model presented in this section provides a possible explanation of deep chlorophyll maxima which, like that shown in Fig. 2, exist in the absence of a DBM.

It may seem that a DCM formed by the mechanism simulated in this model would not be of major ecological significance, since it is due to changes in chlorophyll content and not to phytoplankton abundance. However, this DCM represents a maximum in a species which dominates at depth, and so monopolizes the new nutrients diffusing up from below. Thus, the organisms that comprise this DCM are likely to be responsible for the bulk of the new production (see, e.g., Jenkins and Goldman, 1985).

To investigate this aspect of the model system further, we split the nutrient compartment into new nutrients, N, and recycled or 'old' nutrients, O. The N compartment thus represents nitrate, while O is made up largely of ammonium. When phytoplankton die, they become O nutrients. The parameter R is a remineralization rate—the rate at which recycled nutrients are broken down by bacteria and transformed back into nitrate. In this model, both types of nutrients are taken up indiscriminately by both types of phytoplankton, so that, for a given set of parameters, the division of nutrients into two separate compartments has no effect on the profiles of plankton or of total nutrients. Thus the phytoplankton dynamics of the model are unchanged, and the division allows a distinction to be made between new and regenerated production (Fasham et al., 1990). The 'NOPQ' system is

$$\frac{\partial N}{\partial t} = -\mathrm{G}_P N P \mathrm{e}^{\mathrm{K}z_P} - \mathrm{G}_Q N Q \mathrm{e}^{\mathrm{K}z_Q} + \mathrm{R}O + \kappa \frac{\partial^2 N}{\partial z^2}, \tag{17}$$

$$\frac{\partial O}{\partial t} = -\mathrm{G}_P O P \mathrm{e}^{\mathrm{K}z_P} + \mathrm{D}_P P - \mathrm{G}_Q O Q \mathrm{e}^{\mathrm{K}z_Q} + \mathrm{D}_Q Q - \mathrm{R}O + \kappa \frac{\partial^2 O}{\partial z^2}, \tag{18}$$

$$\frac{\partial P}{\partial t} = \mathrm{G}_P(N+O)P\mathrm{e}^{\mathrm{K}z_P} - \mathrm{D}_P P + \kappa\frac{\partial^2 P}{\partial z^2}, \tag{19}$$

$$\frac{\partial Q}{\partial t} = \mathrm{G}_Q(N+O)Q\mathrm{e}^{\mathrm{K}z_Q} - \mathrm{D}_Q Q + \kappa\frac{\partial^2 Q}{\partial z^2}, \tag{20}$$

with the boundary conditions

$$\frac{\partial N}{\partial z} = \frac{\partial O}{\partial z} = \frac{\partial P}{\partial z} = \frac{\partial Q}{\partial z} = 0 \text{ at } z = 0,$$

$$N = 1, \quad O = P = Q = 0 \text{ at } z = -\infty.$$

In Fig. 11(a), the solution to this system is plotted for the parameter values from Fig. 10 and with $\mathrm{R} = 0.1\ \mathrm{day}^{-1}$. The phytoplankton profiles are the same as in Fig. 10, and the sum of the two types of nutrients yields the total nutrient profile from Fig. 10. The rates of primary production based on new and recycled nutrients by each phytoplankton species are shown in Fig. 11(b). New production is shown as thick lines, recycled production as thin lines, solid lines refer to phytoplankton P, and dashed lines to Q. So, for example, the thick solid line is new production by P, which is just $\mathrm{G}_P NP\mathrm{e}^{\mathrm{K}z_P}$. As expected, the new production is dominated by P.

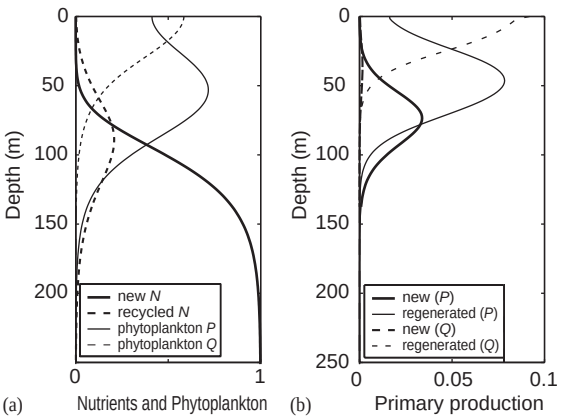

Fig. 11. Results from the NOPQ model, Eqs. (17)–(20). The remineralization rate, R, is $0.1\ \mathrm{day}^{-1}$, and all other parameter values are retained from Fig. 10. (a) Solutions to the model equations; thin lines: phytoplankton P (solid) and Q (dashed), thick lines: new (solid) and recycled (dashed) nutrients. (b) Primary production rates; thin lines: regenerated production by P (solid) and Q (dashed), thick lines: new production by P (solid) and Q (dashed). Units of primary production are nitrogen taken up per day as a fraction of the limiting nitrogen concentration at depth.

The remineralization rate, R, has been found to increase with decreasing light intensity (Olson, 1981), but we take it to be constant here. In addition, a portion of the nitrate which is taken up near the surface has been remineralized within the euphotic zone, and growth based on this portion may not constitute new production in the strictest sense. The likely result of both these simplifications is that we will overestimate the concentration of nitrate in the surface layer, and thus also the proportion of new production carried out by phytoplankton Q. When the 'false' new production is eliminated by allowing remineralization only below the euphotic zone, the main effect is to decrease the rate of new production by phytoplankton Q even further. Much of the nitrate driving new production in the euphotic zone is diffused up from beneath, and so must be balanced by export of nitrogen, in some form, from the euphotic zone. This export is generally attributed to sinking of organic matter, but in the present model, as there is no sinking, the export is carried out by diffusion.

Including sinking in the above model allows for a perhaps more realistic export flux mechanism, and also illustrates the combined effects of surface nitrogen depletion and variation in chlorophyll-to-biomass ratio. With sinking of phytoplankton P, the system becomes

$$\frac{\partial N}{\partial t} = -\mathrm{G}_P NP\mathrm{e}^{\mathrm{K}z_P} - \mathrm{G}_Q NQ\mathrm{e}^{\mathrm{K}z_Q} + \mathrm{R}O + \kappa\frac{\partial^2 N}{\partial z^2}, \tag{21}$$

$$\frac{\partial O}{\partial t} = -\mathrm{G}_P OP\mathrm{e}^{\mathrm{K}z_P} + \mathrm{D}_P P - \mathrm{G}_Q OQ\mathrm{e}^{\mathrm{K}z_Q} + \mathrm{D}_Q Q - \mathrm{R}O + \kappa\frac{\partial^2 O}{\partial z^2}, \tag{22}$$

$$\frac{\partial P}{\partial t} = \mathrm{G}_P(N+O)P\mathrm{e}^{\mathrm{K}z_P} - \mathrm{D}_P P + \kappa\frac{\partial^2 P}{\partial z^2} - \mathrm{W}_P\frac{\partial P}{\partial z}, \tag{23}$$

$$\frac{\partial Q}{\partial t} = \mathrm{G}_Q(N+O)Q\mathrm{e}^{\mathrm{K}z_Q} - \mathrm{D}_Q Q + \kappa\frac{\partial^2 Q}{\partial z^2}. \tag{24}$$

The boundary conditions are

$$\frac{\partial N}{\partial z} = \frac{\partial O}{\partial z} = \mathrm{W}_P P - \kappa \frac{\partial P}{\partial z} = \frac{\partial Q}{\partial z} = 0 \text{ at } z = 0,$$

$$N = 1, \quad P = Q = 0 \text{ at } z = -\infty.$$

Only phytoplankton P sinks, but the resulting surface depletion has an approximately equal impact on both species. Fig. 12 shows the solution for P, Q, and total nutrients ($N + O$) when the sinking rate, W_P, is 1 m day^{-1}, and all other parameter values are preserved from Fig. 10. The maximum concentration of P is reduced to 48% of its former value when sinking is included, while the maximum concentration of Q is reduced to 39% of its former value. The chlorophyll maximum in Fig. 12 is the result of two distinct mechanisms; in addition to the stratification of species with different chlorophyll contents, discussed above, sinking of P gives rise to a DBM, shown in Fig. 12 as the thin solid line, which contributes to the prominence of the DCM.

Because it enhances exchange between different depths, one would expect sinking of phytoplankton to increase the f ratio, that is, the relative amount of new production. Fig. 13 shows the solution to the NOPQ model with sinking of phytoplankton P, and the rates of new and regenerated production. The parameter values are the same as those in Figs. 11 and 12. Comparing Fig. 13(b) with Fig. 11(b), one can see that while the introduction of sinking has caused a reduction in the level of absolute primary production, new production makes up approximately twice as large a fraction of the total—the f ratio has doubled.

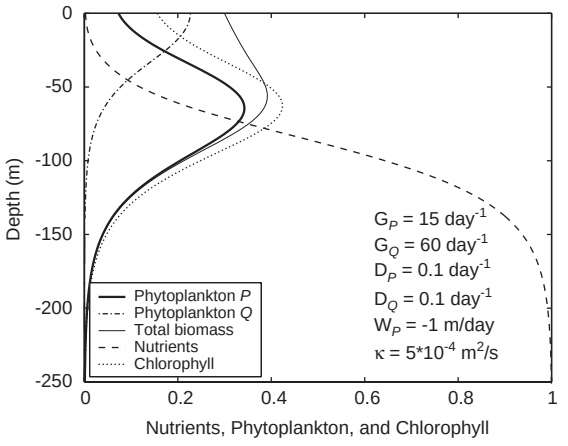

Fig. 12. Solution to the NPQ model with sinking of phytoplankton P (Eqs. (21)–(24)). The total phytoplankton biomass, $P + Q$, is shown as the thin solid line, and total nutrient concentration is the thick dashed line. As in Fig. 10, phytoplankton P has four times the chlorophyll content of phytoplankton Q, and chlorophyll is plotted with arbitrary units.

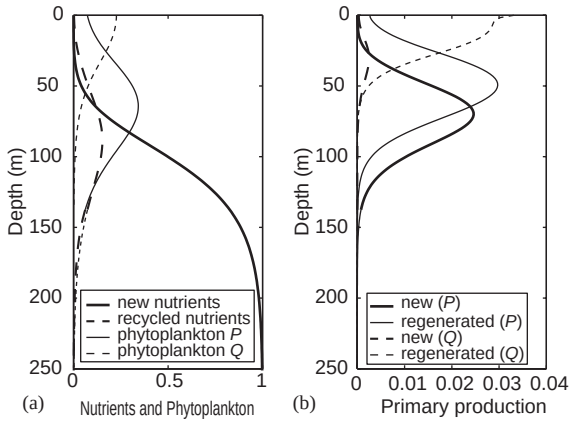

Fig. 13. As in Fig. 11, but with phytoplankton P sinking at 1 m day^{-1}. Note the increase in the ratio of new to regenerated production as compared with Fig. 11.

8. Discussion

Our approach to plankton modeling is to regard nitrogen conservation as an explicit constraint. As primary production in most areas of the oligotrophic ocean is generally considered to be nitrogen limited, biological activity there can be regarded as a competition among species for available nitrogen. Nitrogen may flow between compartments, or from one location to another, but it is not created or destroyed.

The depletion of nitrogen from the upper regions of the euphotic zone caused by sinking of organic matter provides a mechanism for the formation of a DBM in phytoplankton. In a one-dimensional, steady-state, nitrogen-conserving

model of nonmotile phytoplankton, sinking may provide the only reasonable such mechanism. Many authors, dating back to Riley et al. (1949) have included sinking of phytoplankton in their models. However, we suspect that the importance of sinking in determining the distribution of nitrogen with depth has often been under-appreciated. Our models with sinking of nitrogen in various forms demonstrate that the important factor in depleting the euphotic zone of nitrogen (and therefore in forming a DBM) is just that nitrogen sinks. The form of the sinking material, whether phytoplankton, detritus, or any other form, is far less important in determining the vertical structure of the ecosystem. Several authors, notably Steele and Yentsch (1960), have pointed out that a depth-dependent sinking rate can lead to vertical structure in the phytoplankton profile. While one would expect an accumulation of phytoplankton where there is a convergence in sinking rate, we emphasize that the primary importance of sinking in the formation of a deep phytoplankton maximum lies not in its changes with depth, but in its nitrogen-depleting effect on the surface layer.

Models that fail to satisfy the fundamental constraint of nitrogen conservation can produce misleading results. As an example, the model of Varela et al. (1992, 1994), patterned after that of Jamart et al. (1977), does not conserve nitrogen. Though their model does not have an explicit zooplankton compartment, they do include terms representing zooplankton grazing, which removes phytoplankton from the system, and zooplankton excretion, which adds ammonia. As grazing is very much larger than excretion, there is a net removal of nitrogen. At steady state, this loss is balanced by upward diffusion of nitrate from an infinite reservoir at the bottom of the model domain. It is unlikely that Varela et al. (1994) would have written that "…sinking [was] not needed to reproduce the main DCM features…" had they not achieved surface nitrogen depletion by allowing nitrogen to vanish from the euphotic zone.

A parameter study of our NP model with sinking provides information about how parameter values influence the size, shape, and depth of the deep maximum. Perhaps counterintuitively, the value of the phytoplankton growth rate, G, has no influence on the magnitude or shape of the deep maximum, but only on its depth. The depth of the maximum is determined by the growth rate, the sinking rate, and diffusivity, but the dependence is strongest on growth rate. Thus, the magnitude of the maximum is a function of diffusivity and sinking rate, while its depth is largely determined by the growth rate.

Changes in diffusivity with depth, whether these changes occur shallower or deeper than the DBM, do not have a strong effect on its location or magnitude in our NP model. Thus the model does not support the hypothesis, suggested, e.g., by Mann and Lazier (1996), that vertical variation in diffusivity is instrumental in determining the depth of the DBM.

In our models, some factors were found to be of secondary importance in determining the form of the phytoplankton profile. The basic behavior of this profile is captured in a two-compartment model subject to removal of surface nitrogen by sinking. Including additional compartments, such as detritus and zooplankton, does not profoundly affect phytoplankton concentration. The growth rate terms in the models presented here are simple functions of nutrient concentration and light intensity because more complicated forms, when included, were found to introduce only slight changes to the solutions obtained with the simpler forms.

As chlorophyll-to-biomass ratio may change with depth for a number of reasons, a DCM may be caused by a wider variety of mechanisms than a DBM. One such reason is that chlorophyll content varies between species, and species composition is a function of depth. Even though it is not a DBM, a DCM formed in this way may be of ecological interest as the dominant region of new production. That the deep-living species making up the DCM may carry out most of the new production has been suggested before (Venrick, 1993); our NOPQ model illustrates one way this pattern could come about. When sinking of phytoplankton is included in the NOPQ model, a DBM forms, and the f-ratio increases.

The processes highlighted in our models suggest measurements which could test the validity of the

models. If, for example, a DBM arises due to surface nitrogen depletion caused by sinking of phytoplankton or detritus, then a census of total nitrogen, including all the particulate forms and dissolved organic and inorganic nitrogen, should reveal this depletion. The sinking flux of nitrogen in organic materials, which could possibly be measured with sediment traps, should be sufficient to maintain a surface depletion against the upward eddy diffusion of nitrate, which could be inferred from the nitrate profile coupled with eddy diffusivity estimates from dissipation measurements. If a DCM is observed, but measurements determine that surface nitrogen is not depleted, the sinking mechanism is ruled out, and the DCM is likely caused by variation in the chlorophyll-to-nitrogen ratio. In that case, if the 'NPQ' process is important in determining this ratio, the differences between species in chlorophyll content and in the variation of growth rates with light level should be verifiable.

Acknowledgements

We thank Glenn Ierley, Peter Franks, Bill Young, Emmanuel Boss, and three reviewers for many helpful comments. We gratefully acknowledge the support of the National Science Foundation through Grants OCE-0002598, OCE-9819521, and OCE-9819530.

Appendix

We prove that a stable solution to our first model (Eqs. (1) and (2)) exists.

$$\frac{\partial N}{\partial t} = -\mu(N,P,z) + \frac{\partial}{\partial z}\left(\kappa\frac{\partial N}{\partial z}\right),$$

$$\frac{\partial P}{\partial t} = \mu(N,P,z) + \frac{\partial}{\partial z}\left(\kappa\frac{\partial P}{\partial z}\right).$$

Boundary conditions:

$$\frac{\partial N}{\partial z} = \frac{\partial P}{\partial z} = 0 \text{ at } z = 0,$$

$$N = 1, \quad P = 0 \text{ at } z = -\infty.$$

We know that $N + P = 1$, so we can eliminate P from the system

$$P = 1 - N \Rightarrow \frac{\partial N}{\partial t} = -\mu(N,z) + \frac{\partial}{\partial z}\left(\kappa\frac{\partial N}{\partial z}\right),$$

$$\frac{\partial V}{\partial N} \equiv \mu(N,z) \Rightarrow \frac{\partial N}{\partial t} = -\frac{\partial V}{\partial N} + \frac{\partial}{\partial z}\left(\kappa\frac{\partial N}{\partial z}\right).$$

V is determined by μ up to an arbitrary constant. Note that once this constant is chosen, since $N \in [0,1]$, V is bounded for finite μ.

Multiplying by $-\partial N/\partial t$ and integrating over z,

$$-\int_{-\infty}^{0}\left(\frac{\partial N}{\partial t}\right)^2 \mathrm{d}z = \int_{-\infty}^{0}\left[\frac{\partial V}{\partial t} - \frac{\partial}{\partial z}\left(\kappa\frac{\partial N}{\partial z}\right)\frac{\partial N}{\partial t}\right]\mathrm{d}z.$$

Integrating the second term on the right-hand side by parts and applying the BC's, this becomes

$$-\int_{-\infty}^{0}\left(\frac{\partial N}{\partial t}\right)^2 \mathrm{d}z = \frac{\mathrm{d}}{\mathrm{d}t}\int_{-\infty}^{0}\left[V + \frac{1}{2}\kappa\left(\frac{\partial N}{\partial z}\right)^2\right]\mathrm{d}z.$$

As long as N is changing with time, the left-hand side is negative, and the integral on the right-hand side is decreasing. The second term in the integrand is positive, and V is bounded, so the integral on the right-hand side has a minimum value. N can only change until this minimum value has been reached, at which point a stable solution will have been attained.

References

Bishop, J.K.B., 1999. Transmissometer measurement of POC. Deep-Sea Research I 46, 353–369.

Bricaud, A., Morel, A., Prieur, L., 1983. Optical efficiency factors of some phytoplankters. Limnology and Oceanography 28, 816–832.

Criminale, W.O., Winter, D.F., 1974. The stability of steady-state depth distributions of marine phytoplankton. The American Naturalist 108 (963), 679–687.

Cullen, J.J., 1982. The deep chlorophyll maximum: comparing vertical profiles of chlorophyll *a*. Canadian Journal of Fisheries and Aquatic Sciences 39, 791–803.

Cullen, J.J., Lewis, M.R., 1988. The kinetics of algal photoadaptation in the context of vertical mixing. Journal of Plankton Research 10 (5), 1039–1063.

Denman, K., Okubo, A., Platt, T., 1977. The chlorophyll fluctuation spectrum in the sea. Limnology and Oceanography 22, 1033–1038.

Edwards, C.A., Powell, T.A., Batchelder, H.P., 2000. The stability of an *NPZ* model subject to realistic levels of vertical mixing. Journal of Marine Research 58, 37–60.

Falkowski, P., Kiefer, D.A., 1985. Chlorophyll *a* fluorescence in phytoplankton: relationship to photosynthesis and biomass. Journal of Plankton Research 7 (5), 715–731.

Fasham, M.J.R., Ducklow, H.W., McKelvie, S.M., 1990. A nitrogen-based model of plankton dynamics in the oceanic mixed layer. Journal of Marine Research 48, 591–639.

Fennel, K., Boss, E., 2003. Subsurface maxima of phytoplankton and chlorophyll: steady state solutions from a simple model. Limnology and Oceanography 48 (4), 1521–1534.

Franks, P.J.S., Wroblewski, J.S., Flierl, G.R., 1986. Behavior of a simple plankton model with food-level acclimation by herbivores. Marine Biology 91, 121–129.

Jamart, B.M., Winter, D.F., Banse, K., Anderson, G.C., Lam, R.K., 1977. A theoretical study of phytoplankton growth and nutrient distribution in the Pacific Ocean off the northwestern US coast. Deep-Sea Research 24, 753–773.

Jenkins, W.J., Goldman, J.C., 1985. Seasonal oxygen cycling and primary production in the Sargasso Sea. Journal of Marine Research 43, 465–491.

Kitchen, J.C., Zaneveld, J.R.V., 1990. On the noncorrelation of the vertical structure of light scattering and chlorophyll *a* in Case I waters. Journal of Geophysical Research 95 (C11), 20,237–20,246.

Lima, I.D., Olson, D.B., Doney, S.C., 2002. Intrinsic dynamics and stability properties of size-structured pelagic ecosystem models. Journal of Plankton Research 24 (6), 533–556.

Lorenzen, C.J., 1966. A method for the continuous measurement of in vivo chlorophyll concentration. Deep-Sea Research 13, 223–227.

Mann, K.H., Lazier, J.R.N., 1996. Dynamics of Marine Ecosystems. Blackwell Science, Oxford.

Olson, R.J., 1981. Differential photoinhibition of marine nitrifying bacteria: a possible mechanism for the formation of the primary nitrite maximum. Journal of Marine Research 39 (2), 227–238.

Redfield, A.C., Ketchum, B.H., Richards, F.A., 1982. The influence of organisms on the composition of seawater. In: Hill, M.N. (Ed.), The Sea, Vol. 2. Wiley, New York, pp. 26–77.

Riley, G.A., Stommel, H., Bumpus, D.F., 1949. Quantitative ecology of the plankton of the western North Atlantic. Bulletin of the Bingham Oceanographic Collection 12 (3), 1–169.

Steele, J.H., 1974. The Structure of Marine Ecosystems. Harvard University Press, Cambridge.

Steele, J.H., Yentsch, C.S., 1960. The vertical distribution of chlorophyll. Journal of the Marine Biological Association of the United Kingdom 39, 217–226.

Varela, R.A., Cruzado, A., Tintoré, J., Ladona, E.G., 1992. Modelling the deep-chlorophyll maximum: a coupled physical–biological approach. Journal of Marine Research 50, 441–463.

Varela, R.A., Cruzado, A., Tintoré, J., 1994. A simulation analysis of various biological and physical factors influencing the deep-chlorophyll maximum structure in oligotrophic areas. Journal of Marine Systems 5, 143–157.

Venrick, E.L., 1993. Phytoplankton seasonality in the central North Pacific: the endless summer reconsidered. Limnology and Oceanography 38, 1135–1149.

Venrick, E.L., McGowan, J.A., Mantyla, A.W., 1973. Deep maxima of photosynthetic chlorophyll in the Pacific Ocean. Fishery Bulletin (US) 71, 41–52.

Winn, C.D., Campbell, L., Christian, J.R., Letelier, R.M., Hebel, D.V., Dore, J.E., Fujieki, L., Karl, D.M., 1995. Seasonal variability in the phytoplankton community of the North Pacific Subtropical Gyre. Global Biogeochemical Cycles 9 (4), 605–620.

Yentsch, C.S., Yentsch, C.M., 1979. Fluorescence spectral signatures: the characterization of phytoplankton populations by the use of excitation and emission spectra. Journal of Marine Research 37, 471–483.

Young, W.R., 2001. Reproductive pair correlations and the clustering of organisms. Nature 412, 328–331.